

New Scanning Probe Techniques for Analyzing Organic Photovoltaic Materials and Devices

*Rajiv Giridharagopal, Guozheng Shao, Chris Groves, and David S. Ginger
Department of Chemistry, University of Washington, Seattle, WA 98195, USA*

Abstract

Organic solar cells hold promise as an economical means of harvesting solar energy due to their ease of production and processing. However, the efficiency of such organic photovoltaic (OPV) devices is currently below that required for widespread adoption. The efficiency of an OPV is inextricably linked to its nanoscale morphology. High-resolution metrology can play a key role in the discovery and optimization of new organic semiconductors in the lab, as well as assist the transition of OPVs from the lab to mass production. We review the instrumental issues associated with the application of scanning probe microscopy techniques such as photoconductive atomic force microscopy and time-resolved electrostatic force microscopy that have been shown to be useful in the study of nanostructured organic solar cells. These techniques offer unique insight into the underlying heterogeneity of OPV devices and provide a nanoscale basis for understanding how morphology directly affects OPV operation. Finally, we discuss opportunities for further improvements in scanning probe microscopy to contribute to OPV development. All measurements and imaging discussed in this application note were performed with an Asylum Research MFP-3D-BIO™ Atomic Force Microscope.

Introduction

OPV materials are an emerging alternative technology for converting sunlight into electricity. OPVs are potentially very inexpensive to process, highly scalable in terms of manufacturing, and

compatible with mechanically flexible substrates. In an OPV device, semiconducting polymers or small organic molecules are used to accomplish the functions of collecting solar photons, converting the photons to electrical charges, and transporting the charges to an external circuit as a useable current.¹⁻³

At present, the most intensely-studied and highest-performing OPV systems are those that employ bulk heterojunction (or BHJ) blends as the active layer, with NREL-certified power conversion efficiencies improving seemingly monthly, and currently standing at 6.77%.⁴ In a bulk heterojunction blend, the donor and acceptor material are typically mixed in solution, and the mixture is then coated on the substrate to form the active layer. The donor/acceptor pair can consist of two different conjugated polymers, but it is often a conjugated polymer (donor) and a soluble fullerene derivative (acceptor).^{5,6} The illustration in Figure 1a shows a typical BHJ-based OPV device architecture.

Despite the advances of the last few years, the efficiencies of OPVs are still below the level needed for industrial viability. The path towards improved OPV efficiency appears straightforward and researchers are actively working on goals such as better coverage of the solar spectrum to increase current, and tailored energy levels of the donors and acceptors to gain higher open circuit voltages. However, these otherwise straightforward problems in materials synthesis are complicated by the fact that the texture, or morphology, of the

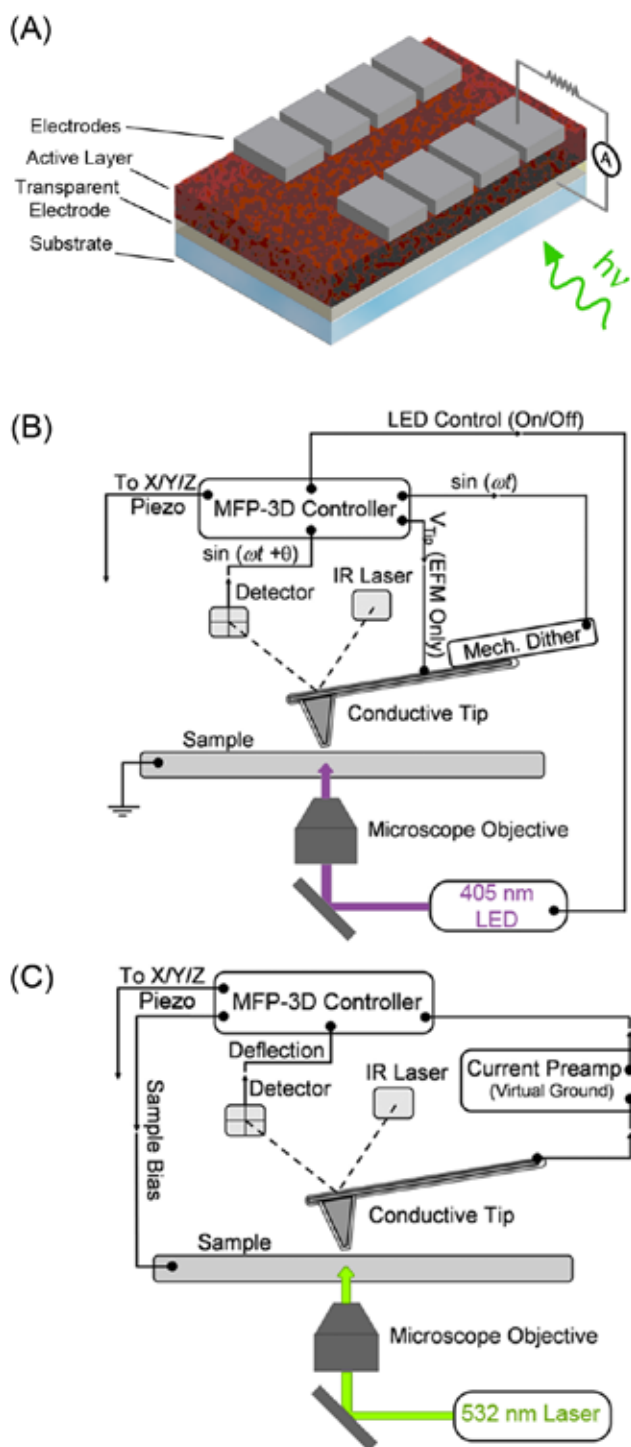


Figure 1. (A) Schematic of a typical bulk heterojunction organic photovoltaic device. Schematic diagrams of the (B) trEFM and (C) pcAFM experimental setups based on Asylum Research's MFP-3D-BIO™ AFM System.

donor acceptor blend – which is sensitive to the exact conditions of how the blend was processed into a thin film – has a dramatic effect on the performance of OPVs.¹ The importance of morphology arises from the competing demands of a number of microscopic processes. First, when light is absorbed in an organic semiconductor, the energy produces a neutral quasiparticle, or exciton, rather than free charge carriers. In most organic solar cells, the exciton is typically dissociated into free charges at the interface between two different organic semiconductors with different electron affinities, hence the widespread use of donor/acceptor blends. However, while the active layer of an organic solar cell needs to be ~100-200nm thick to absorb most of the incident light, the diffusion length of an exciton is ~10nm,^{7,8} and thus the donor and acceptor materials must be mixed on this length scale yield an efficient device.

Analysis of this nanoscale morphology requires high-resolution spatial mapping of the active layer, particularly using scanning probe techniques such as atomic force microscopy (AFM) and its various extensions. Scanning probe microscopy is especially useful because of the ability to image at resolutions approaching the ~10-100nm scale of the domains observed in common OPV materials. Several groups have, for example, analyzed OPV systems using AFM,^{9,10} conducting AFM,^{11,12} electrostatic force microscopy (EFM),¹¹ and scanning Kelvin probe microscopy (SKPM).¹³⁻¹⁶ Optical variations such as near-field scanning optical microscopy (NSOM)^{17,18} and tunneling luminescence-based AFM¹⁹ have also been used to probe OPV blend morphology.

We have recently reviewed the broad use of scanning probe microscopy in the field of organic electronics²⁰ and identified specific areas of nanoscale physics that are important to OPV operation.²¹ In this article, we take a more practical turn and discuss the experimental challenges and opportunities associated with two different AFM techniques, photoconductive AFM (pcAFM)^{22,23} and time-resolved EFM (trEFM)²⁴ that have been used help understand how morphology impacts OPV performance.

trEFM is a non-contact technique that utilizes time-resolved measurements on OPV layers to

analyze the local variations in photoinduced charge generation, collection, and discharge, while pcAFM is a contact-mode method that measures the photocurrent directly to obtain useful information of the local morphology and its relation to the local photoresponse. Figure 1b and 1c show a schematic diagram of the instrumentation used in trEFM and pcAFM. In our lab, we have implemented both techniques using Asylum Research's MFP-3D-BIO AFM coupled to a Nikon TE2000-U inverted optical microscope and controlled using a custom code suite written in Igor (WaveMetrics, Inc.), the scientific software environment used by Asylum Research's AFMs. The system is mounted on an optical breadboard to accommodate external optics (Thor Labs) and is supported by a passive vibration isolation stage (Minus K Technology). Neutral density (ND) filters allow us to adjust the illumination intensity in both techniques. The entire system is housed within a plywood box with copper mesh shielding and acoustic-damping foam. In order to protect potentially air-sensitive samples from photo-oxidation, we use an Asylum Research sealed fluid cell. Originally designed for imaging biological samples under liquid, the design permits the loading of sensitive samples into the cell in a glovebox and allows us to perform measurements while purged with dry nitrogen. This approach obviates the need to install the entire AFM/optical system in a glovebox.

Time-Resolved Electrostatic Force Microscopy (trEFM)

Before discussing the specifics of trEFM, we will first briefly review steady-state EFM. More detailed descriptions of conventional steady-state EFM can be found elsewhere.^{25,26} EFM is a form of AC mode imaging. While most AFM users are familiar with more common forms of AC mode imaging that exploit van der Waals interactions between the tip and the sample to image sample topography (e.g. "intermittent contact mode AFM") EFM makes use of the fact that the cantilever's oscillatory motion is also sensitive to longer-range electrostatic interactions between the tip and sample. In one common EFM imaging mode, these electrostatic interactions are monitored by measuring their effect on cantilever resonance frequency while the cantilever is made to vibrate some distance ($\sim 10\text{nm}$) above the sample

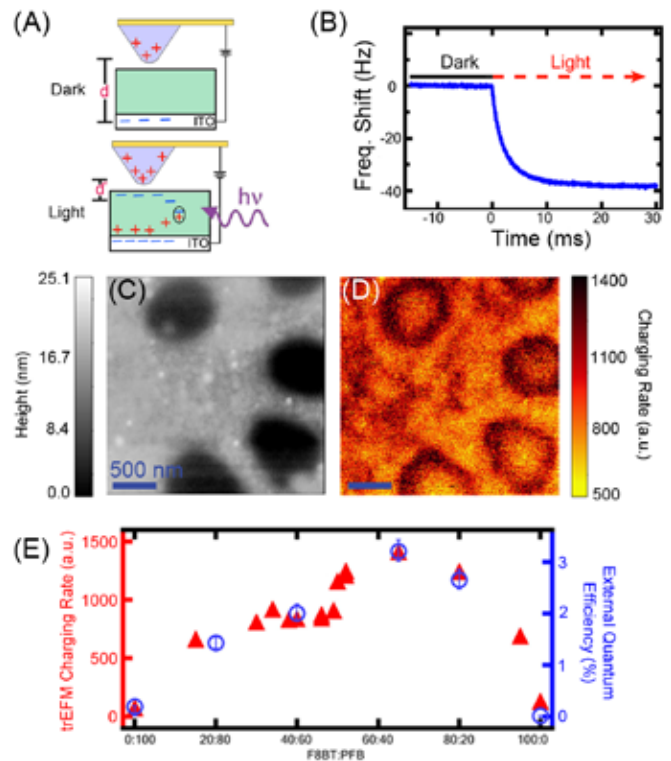


Figure 2. (A) Schematic depiction of how photogenerated charge carriers cause an increase in the capacitive gradient and a change in the surface potential and thus a shift in the resonance frequency. The time rate of change in this shift is what is measured by trEFM. (B) Representative plot of the resonance frequency shift versus time following photoexcitation. At time $t=0$ ms, the LED is turned on, causing an exponential decay in the frequency shift. By finding the time constant of this decay we can extract a relative charging rate. (C) Topography and (D) charging rate image for the same area of a PFB:F8BT sample, dissolved in xylenes with 1:1 composition. (E) Spatially-averaged charging rates in films with different PFB:F8BT ratios are quantitatively consistent with the trend exhibited by EQE measurements. Images reproduced from Ref. 24 with permission of Macmillan Publishers Ltd.

surface. The interactions with the surface at this distance are dominated by local electrostatic force gradients, and the shift in cantilever resonance frequency is proportional to both the local capacitive gradient and the potential difference between the tip and the sample. The frequency shift (f) can be written as:²⁷

$$f = \frac{\partial^2 C}{\partial z^2} (V_{tip} - V_{sample})^2. \quad (1)$$

Here, C is the capacitance, z is the relative tip height, V_{tip} is the voltage applied to the tip, and V_{sample} is the local potential in the sample. In a typical steady-state EFM experiment, a line is scanned in AC mode to record the sample

topography; the tip is then raised a preset distance (for example 20nm) to beyond the range of the short-range van der Waals forces, and the shift in the resonant frequency of the cantilever is measured while a voltage is applied between the tip and sample.

While conventional EFM has been useful in the characterization of a variety of static or quasi-static processes in organic electronic devices,^{11,28} parameters such as surface potential and capacitive gradient fail to provide direct information about the local efficiency of a thin-film solar cell. To address this limitation, we have extended the capability of EFM to enable the study of time-dependent phenomena at sub-ms time scales using trEFM. With trEFM, we can measure the transient behavior in the electrostatic force gradient. Specifically, in our present implementation, we monitor the time-dependent frequency shift in Equation 1 that may result, for instance, from the rapid accumulation of photogenerated charge in a solar cell following illumination, or the fast trapping and detrapping kinetics of charge carriers on sub-ms time scales.

Figure 2a depicts the operation of a trEFM experiment to measure photogenerated charge. In the dark, the semiconductor slab is mostly depleted of charge carriers. The sample is then illuminated with a light pulse and the photoexcitation of the OPV material generates charge carriers. Due to the applied voltage on the tip (in our experiments typically 5-10V), these photogenerated charge carriers migrate to opposite sides of the active layer. The resulting accumulation of charge changes the capacitance and electrostatic force gradient, in turn causing a resonance frequency shift according to Equation 1. By continuously measuring f with $\sim 100\mu\text{s}$ time resolution, we are able to record a charging curve and determine the local charging rate in the material (Figure 2b). While the ability to study dynamic processes is an obvious advantage of trEFM, we have found that another significant advantage of trEFM is that it appears to be less sensitive to tip contamination than conventional EFM or SKPM. We attribute this added robustness to the fact that trEFM measures a *rate of change* rather than an absolute value and so is less sensitive to contamination and consequently is a more repeatable and robust technique.

In our experiments we often use commercial Pt-coated cantilevers (such as Budget Sensors Electric Tap-300G) with spring constant $k \sim 40\text{N/m}$ and resonance frequency $f \sim 300\text{kHz}$. We photoexcite the sample with illumination pulses from LEDs operating at different wavelengths depending on the absorption properties of the sample. For our studies of polyfluorene polymers, we typically use a 405nm LED (LEDtronics L200CUV405-8D16). trEFM is sensitive enough that low-intensity LED illumination, equivalent to 1 Sun or less, is sufficient to produce a useful signal. Attenuation of the light intensity using various ND filters can be used to adjust the total charging time so that it is long enough to be resolved cleanly, but fast enough to make repeated measurements tractable.

In order to generate an image, we pulse the LED at each position on the sample and then record the resulting frequency shift as a function of time, resulting in plots such as that in Figure 2b. An exponential decay function is then fit to the decay of the frequency shift, and this decay constant relates to the photocurrent we wish to measure. We repeat this process for every pixel to generate simultaneous charging rate and topography images. Because the charging process is relatively fast, a 256×256 resolution trEFM image takes about twenty minutes to acquire, which is comparable to standard SKPM techniques. The ability to record the cantilever motion with faster time resolution, which should be possible with the new generation of AFM hardware, would allow the use of higher intensity light pulses and make imaging even faster.

As one example of the capabilities of this technique, we have used trEFM to explore the photoinduced charging behavior in all-polymer OPV blends,²⁴ in this case poly(9,9'-dioctylfluorene-co-benzothiadiazole) (F8BT) and poly(9,9'-dioctylfluorene-co-bis-N,N'-phenyl-1,3-phenylenediamine) (PFB). We chose PFB:F8BT blends as a model system because of the wide literature discussing the effects of processing and blend morphology on their performance. By comparing the topography (Figure 2c) with the charging rate image (Figure 2d), we can analyze the relationship between charging behavior and the local PFB:F8BT film composition. We have

confirmed the utility of trEFM as an analytical technique by showing that the spatially-averaged local charging rate and the measured external quantum efficiency (EQE) are correlated for a wide range of blend ratios (Figure 2e). *This is an exciting result – with only a single calibration factor, a trEFM image of a polymer blend can be used to accurately predict the efficiency of the polymer solar cell that will be fabricated from a particular film.* One can imagine using such a method both to screen new materials in the lab, or as a rapid quality control diagnostic in a production facility. Additionally, we note that it is possible to use trEFM to monitor other quantities of interest, such as spatially-correlated charge trapping and detrapping.

In order to gauge the utility of trEFM in analyzing such materials, it is necessary to determine the spatial and time resolution limits. We estimate the spatial resolution using the data in Figure 3a, where a PFB:F8BT blend is partially removed to expose the underlying substrate (indium tin oxide, ITO) and a charging rate image acquired. Since photoinduced charging does not take place on bare ITO, we can estimate the lateral resolution by determining the point where charging decreases across the polymer-ITO interface. The charging rate at the interface is half that over the polymer. Approximately 90nm away from the interface, the charging rate is 80% of the normal value; this implies a lateral resolution on the order of ~100nm is attainable using trEFM. The corresponding charging rate image and the linear section depicted in the plot are also shown. By applying voltage pulses to a metallic substrate, we can also determine the time resolution of our current apparatus. In Figure 3b, we apply voltage pulses separated by 100 μ s and 50 μ s. At 100 μ s we can clearly observe distinct pulses, but at 50 μ s the time resolution limit of the setup results in an overlap of signals, this is consistent with our experience resolving charging rates on actual polymer films. Based on such data, we claim that trEFM has a spatial/time resolution of ~100nm/~100 μ s, respectively. Improvements in time-resolution beyond the current 100 μ s limit would not only allow us to image faster and better study local carrier dynamics (trapping, transport, detrapping) on shorter time scales, but it would also enable the

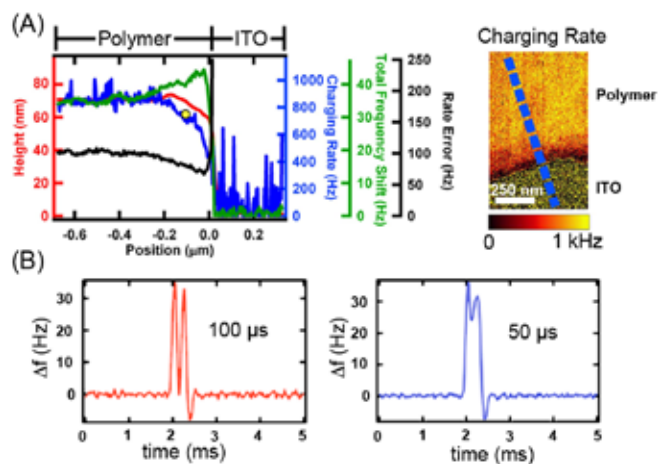


Figure 3. (A) Line traces of the height, charging rate, frequency shift magnitude, and charging rate fit error at the polymer-ITO interface. Data were taken along the area indicated in the corresponding charging rate image (right). The charging rate decreases to 80% the typical polymer charging rate value approximately 90nm from the polymer-ITO interface, as indicated by the yellow circle. (B) Time-resolved voltage pulses on an ITO sample, separated by 100 μ s (left) and 50 μ s (right). The 100 μ s data indicates the time resolution of trEFM; the 50 μ s-separated pulses cannot be clearly-resolved by the current instrumentation. Images A, B reproduced from Ref. 24 with permission of Macmillan Publishers Ltd.

study of more highly performing polymer:fullerene blends without significant attenuation of the LED pump pulse (which can cause additional experimental complications).

Photoconductive Atomic Force Microscopy (pcAFM)

Macroscopic characterization of device parameters such as open circuit voltage, short circuit current and fill factor provide information about overall device performance; however, on the microscopic level, it can be difficult to explain how these parameters are affected by various processing conditions and blend morphologies without direct measurements that can correlate the local electronic properties of the film with local structural features.

Thus, in addition to trEFM, we have used photoconductive AFM (pcAFM) as a complementary tool for the microscopic characterization of heterogeneous OPV films. A relative of conductive AFM (cAFM), pcAFM records local photocurrents directly in contact mode, essentially by using a metalized AFM probe as the top contact to form a nanoscale solar cell. In pcAFM, we typically use focused laser illumination to photoexcite the

sample. The small collection area leads to a small photocurrent, and even high-quality devices with external quantum efficiencies over 50%, we find it beneficial to use high-intensity illumination to improve signal to noise. For instance, a green laser (Crystal Laser GCL-005L, 5mW, 532nm, see Figure 1c) is focused to a diffraction-limited spot on the sample and aligned with the tip; after attenuation, the laser intensity, and therefore the expected sample damage, is often comparable to that in confocal microscopy experiments on biological samples. We also use blue and red lasers as required to match the absorption spectrum of the material being studied. Contact AFM tips with metal overall coating, usually Au (Budget Sensors, ContE-GB, $k \sim 0.2\text{N/m}$), are used for measurement. A small setpoint value is used to minimize destruction of the polymer layer whilst also to keep the conductive coating free from surface contamination. Perhaps one of the most significant practical challenges to using pcAFM is obtaining a good electrical image without causing significant damage to the sample. Patience, and a willingness to sacrifice many AFM cantilevers in the name of science are often necessary.

With pcAFM, the photocurrent measured at a given location reflects the local charge generation properties. At 0 V, this current represents the short-circuit current; it is also possible to record local I-V curves at each point by varying the voltage. We have performed pcAFM on typical polymer/fullerene active layers such as poly(2-methoxy-5-(3',7'-dimethyloctyl-oxy)-1,4-phenylene vinylene) (MDMO-PPV) or poly(3-hexylthiophene) (P3HT) mixed with fullerene derivative (6,6)-phenyl-C61-butyric acid methyl ester (PCBM). We observed microscopic heterogeneity in both topography and short-circuit photocurrent, even in the most efficient MDMO-PPV/PCBM solar cells.²² The variation in photocurrent in otherwise topographically similar areas implies different sub-surface compositions. More recently, we used further pcAFM measurements on P3HT:PCBM samples with different processing conditions to study the underlying morphological contribution to changes in device performance. Annealing a deposited film is a common processing step to improve the efficiency of the device.²⁹ Using pcAFM, we were able to directly observe the relationship between

photocurrent distribution and annealing, namely the increase in both average and peak photocurrent with increased annealing time.²³ For example, in Figure 4a and 4b we show the topography and corresponding short-circuit photocurrent for a P3HT:PCBM film annealed for 10 minutes. As with the MDMO-PPV:PCBM samples, local variations in photocurrent are evident within topographically featureless areas.

As with trEFM, we can assess the quantitative relationship between the pcAFM current information in characterizing OPV efficiency by correlating the spatially-averaged photocurrent in pcAFM data with EQE measurements on the same materials. As can be seen in Figure 4c, photocurrent measurements derived via pcAFM follow the same qualitative trend as the efficiencies obtained from the macroscopic devices. This result suggests that pcAFM can probe the microscopic underpinnings of macroscopic device performance. The pcAFM data acquired can then be useful to extract electron and hole current and mobility from OPV devices and could even be used as a tool to select optimal blends and processing conditions. However, it is important to emphasize that while the qualitative trends between the pcAFM data and EQE are generally in good agreement, we often find quantitative differences between the local pcAFM averages and the bulk device properties. This is not entirely surprising given that we are using high work function tips (Au, Pt) and that contact effects are expected to play some role in the current extraction. Indeed, it is for this reason that we believe pcAFM data generally correlates better with macroscopic performance for a fixed blend ratio than it does across a wide range of donor/acceptor concentrations,²² and the importance of the tip workfunction and any associated injection/extraction barrier should always be kept in mind when analyzing pcAFM data.

Summary and Outlook

The BHJ morphology upon which OPVs rely is extremely complex. The mixing of an electron donor and acceptor in a common solution, followed by spin coating, yields a morphology that has features on a variety of length scales. These features in turn affect the ability of the device to split excitons and the ability of the resulting charges

to navigate a route through the film to emerge as useful photocurrent. As a result, the performance of OPVs is inherently a local property. Measurements on bulk devices that are several mm² in area will implicitly involve a great deal of averaging of the device properties and much of the local microscopic detail will subsequently be lost.

The techniques we have described here are extensions to the conducting-AFM measurement made with an Asylum Research MFP-3D-BIO. These in turn have allowed use to make measurements of the morphology, electrical and optical properties of BHJs all on the nanoscale, and, crucially, on the same area of the device. As a result we have been able to make significant steps forward in our understanding of how even well-characterized OPV systems operate in terms of the local morphology.

It seems that there is much room for further advancement. For example improvements in time resolution in trEFM beyond the current 100 μ s limit, for example using newer generation equipment with higher bandwidth, could open up further time-resolved experiments on different systems such as polymer:fullerene devices as well as improve the throughput of the technique. Coupling broad spectrum illumination with the pcAFM and trEFM setups would also allow for spectral analysis of optoelectronic behavior. Further pcAFM work is currently underway in several groups using lower work function tips so as to avoid some of the limitations discussed above and perhaps achieve better quantitative agreement between EQE and spatially-averaged photocurrent on different donor/acceptor blend ratio devices.

While the techniques here are presented in the context of OPV morphology, it should be stressed that they can also be useful in other photoactive technologies. For example, solid-state dye sensitized solar cells³⁰ or composite photocatalysts³¹ are expected to exhibit local heterogeneity that would ultimately impact electrical performance. trEFM and pcAFM therefore provide ideal tools for characterizing these systems.

Acknowledgments

The authors thank Kevin Noone for assistance with the first figure and Obadiah Reid for helpful discussion. This review is based in part on

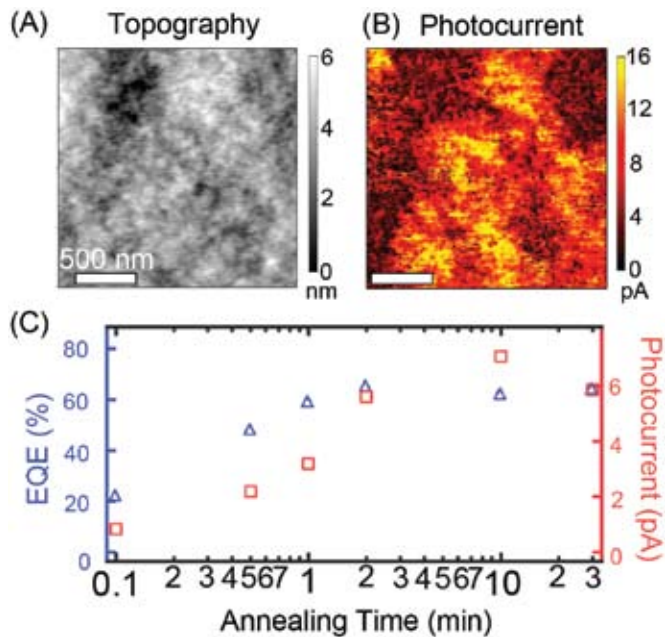


Figure 4. Microscopic heterogeneity in (A) topography and (B) photocurrent on P3HT/PCBM blends. 2 μ m scan. (C) Correlation between spatially-averaged photocurrent measured via pcAFM and EQE measurements for P3HT/PCBM blends annealed for different lengths of time again indicate that pcAFM data are qualitatively consistent with expected device performance. Images reproduced from Ref. 23 with permission of the American Chemical Society.

work supported by the NSF (DMR-0120967 and DMR-0449422), AFOSR, DOE, and ONR. D.S.G. also thanks the Camille Dreyfus Teacher-Scholar Awards program and the Alfred P. Sloan foundation for support.

1. Chen, L., Hong, Z., Li, G. and Yang, Y. Recent progress in polymer solar cells: Manipulation of polymer: Fullerene morphology and the formation of efficient inverted polymer solar cells. *Adv. Mater.* **21**, 1 (2009).
2. Coakley, K. M. and McGehee, M. D. Conjugated polymer photovoltaic cells. *Chem. Mater.* **16**, 4533 (2004).
3. Guenes, S., Neugebauer, H. and Sariciftci, N. S. Conjugated polymer-based organic solar cells. *Chem. Rev.* **107**, 1324–1338 (2007).
4. Chen, H.-Y. et al. Polymer solar cells with enhanced open-circuit voltage and efficiency. *Nature Photonics* **3**, 649 (2009).
5. Morita, S., Zakhidov, A. A. and Yoshino, K. Doping effect of buckminsterfullerene in conducting polymer: Change of absorption spectrum and quenching of luminescence. *Sol. St. Comm.* **82**, 249 (1992).
6. Sariciftci, N. S., Smilowitz, L., Heeger, A. J. and Wudl, F. Photoinduced electron transfer from a conducting polymer to buckminsterfullerene. *Science* **258**, 1474 (1992).

7. Scully, S. R. and McGehee, M. D. Effects of optical interference and energy transfer on exciton diffusion length measurements in organic semiconductors. *J. Appl. Phys.* **100**, 034907 (2006).
8. Shaw, P. E., Ruseckas, A. and Samuel, I. D. W. Exciton diffusion measurements in poly(3-hexylthiophene). *Adv. Mater.* **20**, 3516 (2008).
9. Hoppe, H. et al. Nanoscale morphology of conjugated polymer/fullerene-based bulk-heterojunction solar cells. *Adv. Func. Mater.* **14**, 1005 (2004).
10. Moule, A. J. and Meerholz, K. Controlling morphology in polymer-fullerene mixtures. *Adv. Mater.* **20**, 240 (2008).
11. Douhéret, O. et al. High resolution electrical characterization of organic photovoltaic blends. *Micro. Eng.* **84**, 431 (2007).
12. Leever, B. J. et al. Spatially resolved photocurrent mapping of operating organic photovoltaic devices using atomic force photovoltaic microscopy. *Appl. Phys. Lett.* **92**, 013302 (2008).
13. Chiesa, M. et al. Correlation between surface photovoltage and blend morphology in polyfluorene-based photo-diodes. *Nano Lett.* **5**, 559 (2005).
14. Hoppe, H. et al. Kelvin probe force microscopy study on conjugated polymer/fullerene bulk heterojunction organic solar cells. *Nano Lett.* **5**, 269 (2005).
15. Maturová, K., Kemerink, M., Wienk, M. M. and Charrier, D. S. H. Scanning kelvin probe microscopy on bulk heterojunction polymer blends. *Adv. Func. Mater.* (2009).
16. Palermo, V., Palma, M. and Samori, P. Electronic characterization of organic thin films by Kelvin probe force microscopy. *Adv. Mat.* **18**, 145-164 (2006).
17. McNeill, C. R., Frohne, H., Holdsworth, J. L. and Dastoor, P. C. Near-field scanning photocurrent measurements of polyfluorene blend devices: directly correlating morphology with current generation. *Nano Lett.* **4**, 2503 (2004).
18. Riehn, R. et al. Local probing of photocurrent and photoluminescence in a phase-separated conjugated-polymer blend by means of near-field excitation. *Adv. Func. Mater.* **16**, 469 (2006).
19. Romero, M. J., Morfa, A. J., Reilly III, T. H., van de Lagemaat, J. and Al-Jassim, M. Nanoscale imaging of exciton transport in organic photovoltaic semiconductors by tip-enhanced tunneling luminescence. *Nano Lett.* **9**, 3904 (2009).
20. Pingree, L. S. C., Reid, O. G. and Ginger, D. S. Electrical scanning probe microscopy on active organic electronic devices. *Adv. Mater.* **21**, 19 (2009).
21. Groves, C., Reid, O. G. and Ginger, D. S. Heterogeneity in polymer solar cells: local morphology and performance in organic photovoltaics studied with scanning probe microscopy. *Acc. Chem. Res.*, in press.
22. Coffey, D. C., Reid, O. G., Rodovsky, D. B., Bartholomew, G. P. and Ginger, D. S. Mapping local photocurrents in polymer/fullerene solar cells with photoconductive atomic force microscopy. *Nano Lett.* **7**, 738 (2007).
23. Pingree, L. S. C., Reid, O. G. and Ginger, D. S. Imaging the evolution of nanoscale photocurrent collection and transport networks during annealing of polythiophene/fullerene solar cells. *Nano Lett.* **9**, 2946 (2009).
24. Coffey, D. C. and Ginger, D. S. Time-resolved electrostatic force microscopy of polymer solar cells. *Nat. Mater.* **5**, 735 (2006).
25. Girard, P. Electrostatic force microscopy: principles and some applications to semiconductors. *Nanotechnology* **12**, 485 (2001).
26. Kalinin, S. V. and Bonnell, D. A. in Scanning probe microscopy and spectroscopy: theory, techniques, and applications (ed. Bonnell, D. A.) 205-251 (Wiley-VCH, New York, 2001).
27. Muller, E. M. and Marohn, J. A. Microscopic evidence for spatially inhomogeneous charge trapping in pentacene. *Adv. Mater.* **17**, 1410 (2005).
28. Silveira, W. R. and Marohn, J. A. Microscopic view of charge injection in an organic semiconductor. *Phys. Rev. Lett.* **93**, 116104 (2004).
29. Ma, W., Yang, C. and Heeger, A. J. Spatial Fourier-transform analysis of the morphology of bulk heterojunction materials used in "plastic" solar cells. *Adv. Mater.* **19**, 1387 (2007).
30. Luo, Y., Li, D. and Meng, Q. Towards optimization of materials for dye-sensitized solar cells. *Adv. Mater.* **21**, 1 (2009).
31. Zhong, D. K., Sun, J., Inumaru, H. and Gamelin, D. R. Solar water oxidation by composite catalyst/ α -Fe₂O₃ photoanodes. *J. Am. Chem. Soc.* **131**, 6086 (2009).